JUSTC

Article

http://justc.ustc.edu.cn

Received: November 16, 2021; Accepted: February 09, 2022

# Experimental investigation of dynamic mechanical properties of foamed magnesium oxysulfate cementitious material

Xiaofei Yi[1], Shaohua Wang[1], Yongliang Zhang[1,2] ✉, Di Zhao[1], Xiaoda Cui[3], and Zhijun Zheng[1]

[1]*CAS Key Laboratory of Mechanical Behavior and Design of Materials, Department of Modern Mechanics, University of Science and Technology of China, Hefei 230027, China;*
[2]*Anhui Province Key Laboratory of Green Building and Assembly Construction, Anhui Institute of Building Research & Design, Hefei 230031, China;*
[3]*Shanghai Environment Group Co., Ltd., Shanghai 200050, China*

✉Correspondence: Yongliang Zhang, E-mail: ylz2018@ustc.edu.cn


## Graphical abstract

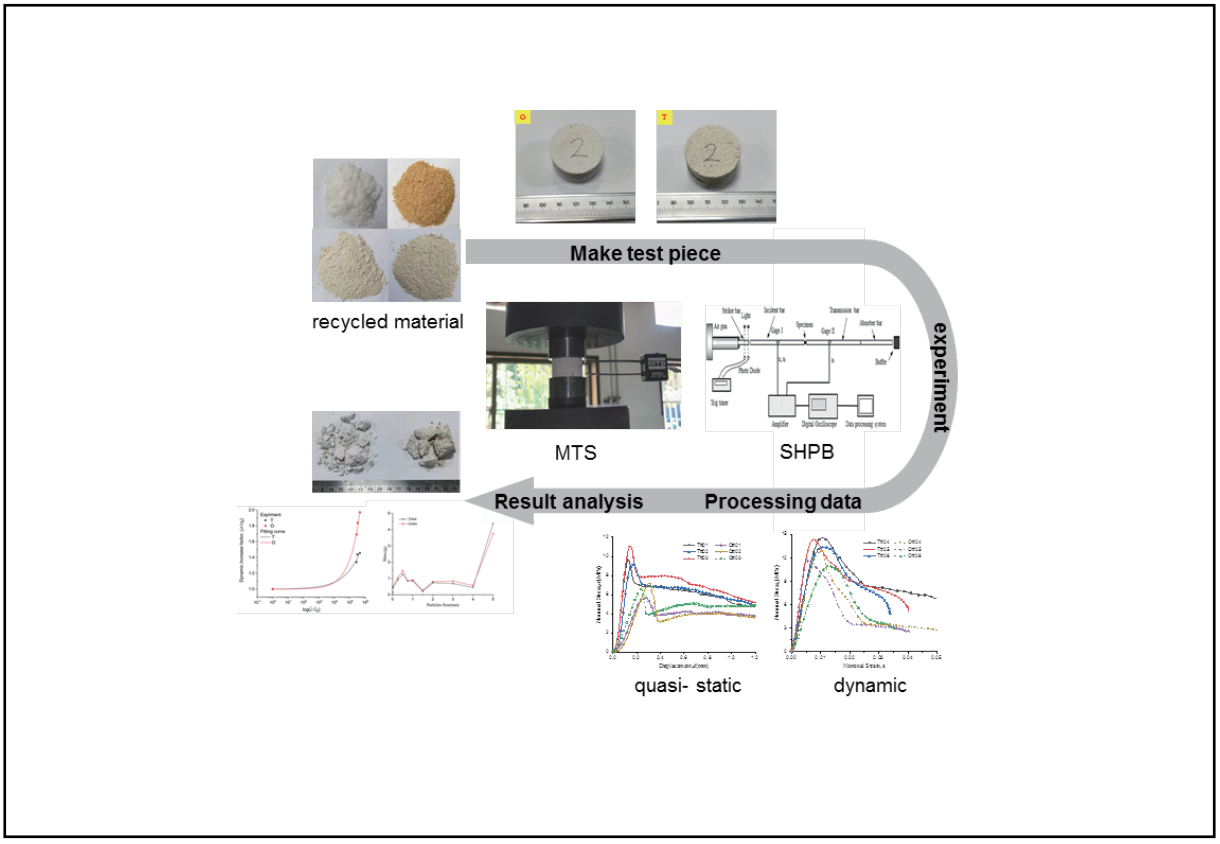


*It shows the research ideas and some important data of this paper.*

## Public summary

■ The internal cavity pore sizes became smaller owing to the addition of recycled materials.

■ The quasi-static strength of the FMOCM was improved, but the strain rate effect was weakened.

■ The FMOCM with solid waste materials show better toughness.

**Citation:** Yi X F, Wang S H, Zhang Y L, et al. Experimental investigation of dynamic mechanical properties of foamed magnesium oxysulfate cementitious material. *JUSTC*, **2022**, 52(4): 6. DOI: 10.52396/JUSTC-2021-0233

JUSTC

Article

http://justc.ustc.edu.cn

Received: November 16, 2021; Accepted: February 09, 2022

# Experimental investigation of dynamic mechanical properties of foamed magnesium oxysulfate cementitious material

Xiaofei Yi[1], Shaohua Wang[1], Yongliang Zhang[1,2] ✉, Di Zhao[1], Xiaoda Cui[3], and Zhijun Zheng[1]

[1]*CAS Key Laboratory of Mechanical Behavior and Design of Materials, Department of Modern Mechanics, University of Science and Technology of China, Hefei 230027, China;*

[2]*Anhui Province Key Laboratory of Green Building and Assembly Construction, Anhui Institute of Building Research & Design, Hefei 230031, China;*

[3]*Shanghai Environment Group Co., Ltd., Shanghai 200050, China*

✉Correspondence: Yongliang Zhang, E-mail: ylz2018@ustc.edu.cn



Cite This: *JUSTC*, **2022**, 52(4): 6 (6pp)

Read Online

**Abstract:** With the rapid reutilization of solid waste materials, it is imperative to investigate the properties of composite materials formed by the addition of solid waste materials. Basic foamed magnesium oxysulfate cementitious material(FMOCM) with and without solid waste materials were studied and compared. This study focused on the internal structures and quasi-static and dynamic mechanical properties of FMOCM. The results showed that the internal cavity structure of the FMOCM underwent significant changes, and the pore sizes became smaller owing to the addition of recycled materials and wood flour, which greatly improved the quasi-static strength of the FMOCM. It was found that the FMOCM had obvious strain rate effects. By comparing the dynamic strength factors, the dynamic strength of the regular FMOCM almost doubled, and the addition of solid waste materials weakened the strain rate effect. Only when the strain rate was lower did the FMOCM with solid waste materials show better toughness compared to the more serious fracture of the regular FMOCM. Furthermore, this study demonstrated the broad application prospects of solid waste materials in magnesium oxysulfide cementitious materials.

**Keywords:** magnesium oxysulfide cementitious; dynamic mechanical properties; strain rate effect; solid waste materials

**CLC number:** TQ31； TB33 **Document code:** A

## 1 Introduction

The recycling of solid waste materials is conducive to the protection of the ecological environment and the sustainable development of resources, and the utilization of recycled materials is one of the key technologies for improving the utilization efficiency of solid waste regeneration. Magnesium oxysulfide cementitious material with high strength, good fire resistance, and low energy consumption is a type of air-hardening ternary cementitious system material. MgO-$MgSO_4$-$H_2O$, composed of lightly burnt MgO and a solution of magnesium oxysulfate heptahydrate ($MgSO_4·7H_2O$), has three common crystal phases: Mg $(OH)_2$, $MgSO_4·7H_2O$, and 3Mg $(OH)_2·MgSO_4·8H_2O$[1–3].

In recent years, suitable additives such as citric acid and citrate[4–9], tartaric acid and tartrate[10], phosphate[11–13], tartaric acid[14], and magnesium oxysulfate cement(MOC) have been developed. Its main hydration products, newly discovered magnesium oxysulfate whiskers with a chemical formula of $5Mg(OH)_2·MgSO_4·7H_2O$, exhibit a higher performance. The mechanical properties of basic magnesium oxysulfate cementitious material(BMSC) have been widely studied as green and environmentally friendly civil engineering materials[15]. Chen et al. prepared a basic foamed magnesium oxysulfate cementitious material (FMOCM) with light calcined magnesia and magnesium oxysulfate heptahydrate with a dry density of 100–500 kg/m$^3$[16]. The effects of the foaming agent on the porosity and mechanical properties of the FMOCM were studied, and its strength, water absorption, and thermal conductivity were measured. Cong et al.[17,18] studied the effects of glass fiber and polypropylene fiber content on the dry density, thermal conductivity, porosity, volumetric water absorption, softening coefficient, and mechanical properties of a FMOCM. However, to date, research on the dynamic mechanical properties of FMOCMs is still lacking.

Currently, magnesia cementitious materials, mainly used in construction projects such as the production of building insulation materials and prefabricated building materials, meet the requirements of building energy efficiency and environmental protection and are expected to become the future core high-performance eco-friendly cement. With urbanization, more solid waste materials are produced that occupy farmland, destroy ecology, and pollute the environment. The use of solid waste materials in FMOCMs has great development potential for replacing traditional building materials. Based on recycled materials, an FMOCM prepared from recycled magnesia cementitious material and wood was developed.

In this study, the basic mechanical properties of an FMOCM were systematically measured. Quasi-static and dynamic compressive strengths were studied to analyze the



DOI: 10.52396/JUSTC-2021-0233

*JUSTC*, **2022**, 52(4): 6

strain rate effect. The differences in the mechanical properties of FMOCMs with/without recycled materials and wood flour were compared. The comparison has practical significance for fully understanding the advantages of FMOCMs in terms of their mechanical properties and expanding their application in the civil engineering industry. Thus, this study provides a foundation for the future development of structural materials for magnesium oxysulfate cementitious systems.

## 2 Experimental tests

### 2.1 Raw materials

Magnesium oxysulfate heptahydrate(Fig. 1a) was obtained from Jiangsu Kouyuan Magnesium Industry Co., Ltd. and contained 99% effective content of $MgSO_4 \cdot 7H_2O$. Wood flour(Fig. 1b) was obtained from the Liannan Yao Autonomous County Jinwen wood processing factory, and its size was less than 1 mm. Light-burned MgO powder(Fig. 1c) from Liaoning Haicheng Magnesite was calcined at 700–1000 °C by Haicheng Qianyuan Refractory Co., Ltd. The fineness of the light-burned MgO powder was 200 mesh. The activity of MgO was more than 63%. The recycled material(Fig. 1d) after abrasion by a sanding machine was the waste material of the MOC manufactured by Ningguo Green New Material Technology Co., Ltd., with a fineness of 200 mesh. The admixture was a polymer complex protein foaming agent and acid modifier based on inorganic acids from Ningguo Green New Material Technology Co., Ltd.

### 2.2 Mixture proportions

First, magnesium oxysulfate was melted and added to water, and brine was prepared with a solution at 26.0 Baumé degrees. Then, the brine, MgO, MOC, recycled material, wood flour, and acid modifier were placed in turn into a mixer in the proportions shown in Table 1. The obtained samples were

(a) Magnesium oxysulfate heptahydrate (b) Wood flour

(c) Light-burned magnesium oxide (d) Recycled material

**Fig. 1.** Photographs of raw materials.

**Table 1.** Mixture proportions(kg/m³).

| | Brine | MgO | Recycled material | Wood flour |
|---|---|---|---|---|
| *T* | 448 | 320 | 100 | 51.2 |
| | $MgSO_4 \cdot 7H_2O$ | | MgO | $H_2O$ |
| *O* | 324.4 | | 1000 | 620.8 |

classified into two categories according to their content. The sample containing recycled material and wood flour was recorded as "*T*," and the sample without solid waste materials was recorded as "*O*". After stirring for 3 to 5 min, a foam machine was used to add foam and stir until the foamed cementitious material was well distributed. Finally, the mixture was poured into a mold and cured under natural conditions for 28 days.

For comparison with the FMOCM with solid waste materials, the regular FMOCM was prepared using the same method, and its main components are listed in Table 1.

### 2.3 Sample preparation

After demolding, the samples were prepared by coring and cutting, and the end faces were polished with a precision of ± 0.05 mm. To obtain the mechanical properties of the FMOCM, quasi-static uniaxial compression tests and split Hopkinson pressure bar(SHPB0 tests were carried out. The quasi-static test sample sizes of the FMOCMs with and without solid waste materials were 50 × 50 × 50 mm and Φ32 × 20 mm, respectively. The SHPB test dimensions were Φ32 × 20 mm as shown in Fig. 2.

The real densities of the FMOCMs with and without solid waste materials calculated by the weight and volume of the sample were 0.77 and 0.64 g/cm³, respectively. The microstructures of the samples were characterized by scanning elec-

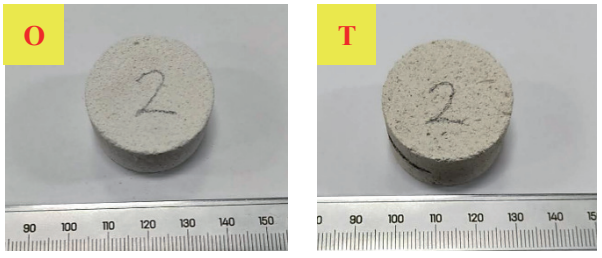


**Fig. 2.** Photographs of SHPB tests samples.

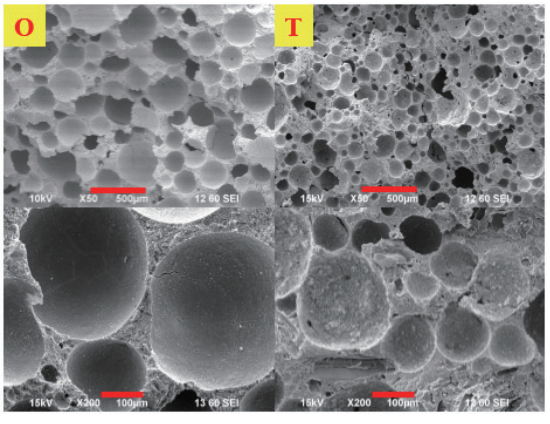


**Fig. 3.** SEM images of FMOCMs.


DOI: 10.52396/JUSTC-2021-0233
*JUSTC*, **2022**, 52(4): 6

tron microscopy(SEM) (JEOL JSM-6390LA, Japan) as shown in Fig. 3.

The SEM image(Fig. 3) shows that the pore microstructure of the regular FMOCM had an average length of 200 μm. With the addition of solid waste materials, the internal pore size decreased to an average length of 100 μm, and the pore wall structure became loose. However, the structure of the matrix material was essentially the same.

### 2.4 Experimental method

Quasi-static uniaxial compression tests were carried out on a material testing machine(MTS810) at the Material Mechanical Properties Test Laboratory of the Engineering Experimental Center of the University of Science and Technology of China with a loading rate of 0.001 $s^{-1}$. Dynamic tests were performed on a SHPB with a diameter of 32 mm as shown in Fig. 4.

The measured signals of the incident, reflected, and transmitted waves are denoted as $\varepsilon_I(t)$, $\varepsilon_R(t)$, and $\varepsilon_T(t)$, respectively, where $t$ is the time. The displacements $u_1$ and $u_2$ of the two end faces of the sample can be expressed as

$$u_1 = \int_0^t c_0 E_1 \mathrm{d}t, \quad u_2 = \int_0^t c_0 E_2 \mathrm{d}t \tag{1}$$

where $c_0$ is the wave velocity of the incident and the transmission bars, $\varepsilon_1$ is the strain of the contact surface between the incident bar and the sample, which includes the incident and reflected pulses, and $\varepsilon_2$is the strain of the contact surface between the transmission rod and the sample, which is only related to the transmission pulse. Therefore, the end-face displacements can be expressed as

$$u_1 = \int_0^t c_0 [\varepsilon_I(t) - \varepsilon_R(t)] \mathrm{d}t, u_2 = \int_0^t c_0 \varepsilon_T(t) \mathrm{d}t \tag{2}$$

The average strain of the sample is

$$\varepsilon(t) = \frac{u_1 - u_2}{L} = \frac{c_0}{L} \int_0^t (\varepsilon_I(t) - \varepsilon_R(t) - \varepsilon_T(t)) \mathrm{d}t \tag{3}$$

where $L$ is the length of the sample. By calculating the derivative of Eq. (3) with respect to time, the outcome is the average strain rate:

$$\dot{\varepsilon}(t) = \frac{c_0}{L} [\varepsilon_I(t) - \varepsilon_R(t) - \varepsilon_T(t)] \tag{4}$$

The force on both ends of the sample can be expressed as

$$P_1(t) = EA[\varepsilon_I(t) + \varepsilon_R(t)] \tag{5}$$

$$P_2(t) = EA\varepsilon_T(t) \tag{6}$$

where $A$ is the cross-sectional area of the incident and transmission bars, and $E$ is the elastic modulus of the bar.

The results show that the average stress in the sample was

$$\sigma(t) = \frac{P_1(t) + P_2(t)}{2A_s} = \frac{EA}{2A_s} [\varepsilon_I(t) + \varepsilon_R(t) + \varepsilon_T(t)] \tag{7}$$

where $A_s$ is the cross-sectional area of the sample.

Eqs. (3), (4), and (7) are the three-wave method of the stress–strain relationship of the sample under a high strain rate measured by the ordinary SHPB experiment, namely,

$$\left.\begin{aligned} \varepsilon(t) &= \frac{c_0}{L} \int_0^t [\varepsilon_I(t) - \varepsilon_R(t) - \varepsilon_T(t)] \mathrm{d}t \\ \dot{\varepsilon}(t) &= \frac{c_0}{L} [\varepsilon_I(t) - \varepsilon_R(t) - \varepsilon_T(t)] \\ \sigma(t) &= \frac{EA}{2A_s} [\varepsilon_I(t) + \varepsilon_R(t) + \varepsilon_T(t)] \end{aligned}\right\} \tag{8}$$

In addition, applying the assumption of uniformity, we obtain

$$\varepsilon_I(t) + \varepsilon_R(t) = \varepsilon_T(t) \tag{9}$$

Substituting Eq. (9) into Eq. (8), we obtain

$$\left.\begin{aligned} \varepsilon(t) &= -\frac{2c_0}{L} \int_0^t \varepsilon_R(t) \mathrm{d}t \\ \dot{\varepsilon}(t) &= -\frac{2c_0}{L} \varepsilon_R(t) \\ \sigma(t) &= \frac{EA}{A_s} \varepsilon_T(t) \end{aligned}\right\} \tag{10}$$

The method of using Eq. (10) to obtain the stress–strain relationship of materials is known as the two-wave method. Owing to the serious dispersion of reflected waves measured by a large-scale SHPB rod, the two-wave method is often used to process experimental data when processing concrete data.

## 3 Results and discussion

### 3.1 Quasi-static mechanical properties

The stress–displacement curves of the FMOCM under quasi-static loading conditions $\dot{\varepsilon}_0$ = 0.001 $s^{-1}$ and the stress–dis-

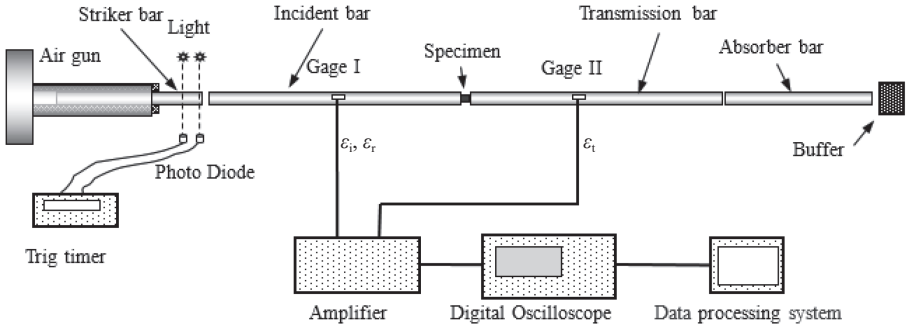


**Fig. 4.** Schematic diagram of SHPB.


DOI: 10.52396/JUSTC-2021-0233
*JUSTC*, **2022**, 52(4): 6

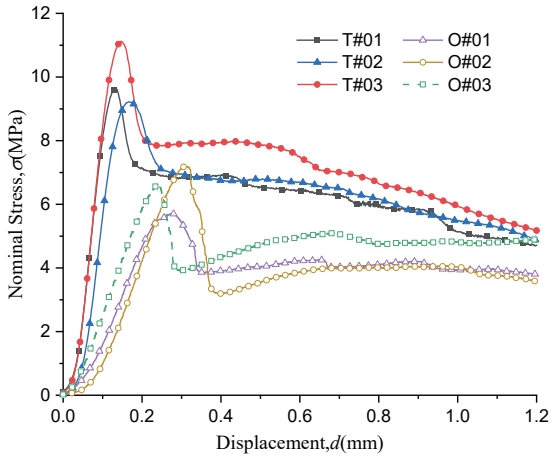


**Fig. 5.** Stress-displacement curves of FMOCMs under quasi-static compression.

**Table 2.** Quasi-static test results.

| Parameter | No. | | | | | |
|---|---|---|---|---|---|---|
| | *T*#01 | *T*#02 | *T*#03 | *O*#01 | *O*#02 | *O*#03 |
| Peak failure strain /$10^{-3}$ | 6.10 | 8.25 | 7.21 | 4.8 | 5.6 | 6.2 |
| Compressive strength /MPa | 9.67 | 9.24 | 11.20 | 6.6 | 5.7 | 7.2 |

placement curves of the FMOCM are shown in Fig. 5, and the compressive strength and peak failure strain can be calculated separately by force and displacement as shown in Table 2. The average compressive strength of the FMOCM with solid waste materials was 10.0 MPa with a 54% increase in contrast with that of the regular FMOCM. Similarly, the average peak strain of the former specimen was 30% higher than that of the latter at failure.

### 3.2 Dynamic mechanical properties

According to the SHPB test results (Table 3) and processed test data, the stress–strain curve of the FMOCMs under different strain rates can be obtained as shown in Fig. 6. It can be seen that the material had a significant strain rate effect, and the dynamic compressive strength of the FMOCM with solid waste materials was stronger than that of the regular FMOCM. For further comparison and analysis of the mechanical properties, the relationship between the dynamic strength and strain rate of the FMOCM was established and normalized based on the quasi-static compressive strength $\sigma_0$ and loading rate $\dot{\varepsilon}_0 = 0.001\ \mathrm{s}^{-1}$ as shown in Fig. 7. The DIF = $\sigma/\sigma_0$ fitting formulas are

$$\mathrm{DIF}^T = 1 + 0.0015(\lg\dot{\varepsilon}/\dot{\varepsilon}_0)^{0.22} \tag{11}$$

$$\mathrm{DIF}^O = 1 + 0.00024(\lg\dot{\varepsilon}/\dot{\varepsilon}_0)^{0.64} \tag{12}$$

The dynamic strength of the regular FMOCM nearly doubled. However, the enhancement in the dynamic strength of the FMOCM with solid waste materials was weaker than that of the regular FMOCM, indicating that the recycled materials and wood flour reduced the strain rate effect of the FMOCM.

The macro fracture of the FMOCM was the result of the internal defect of the original material expansion and penetration of the base material continuously under the action of external factors such as impact load, which eventually led to fracture. There were randomly distributed cavities in the FMOCMs. Under an impact load, the internal failure modes of the FMOCMs varied, such as tensile cracks, shear, crushing, and peripheral shedding.

The fracture characteristics of the SHPB test specimens are shown in Fig. 8. It can be seen that the crushing of the

**Table 3.** Dynamic test results.

| Parameter | No. | | | | | |
|---|---|---|---|---|---|---|
| | *T*#04 | *T*#05 | *T*#06 | *O*#04 | *O*#05 | *O*#06 |
| Average strain rate /$\mathrm{s}^{-1}$ | 490 | 330 | 270 | 440 | 320 | 270 |
| Dynamic compressive strength /MPa | 14.56 | 14.37 | 13.42 | 12.81 | 11.94 | 10.99 |

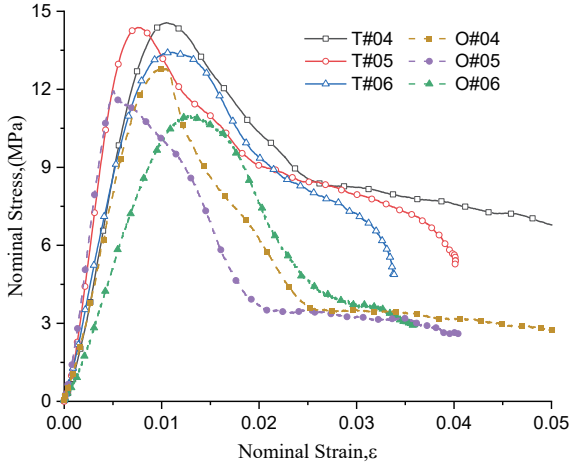


**Fig. 6.** Stress-strain curves of FMOCMs under dynamic compression.

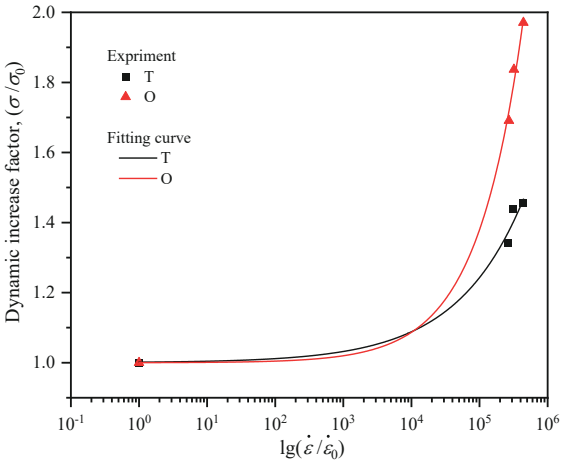


**Fig. 7.** Relationship between normalized dynamic strength and strain rate.


DOI: 10.52396/JUSTC-2021-0233
*JUSTC*, **2022**, 52(4): 6

(a) Regular FMOCM (b) FMOCM with solid waste

**Fig. 8.** Fracture characteristics under dynamic compression.

FMOCM with solid waste materials was more sufficient than that of the regular FMOCM under a uniaxial impact load with the strain rate of 270 $s^{-1}$. When the strain rate was greater than 400 $s^{-1}$, the samples with and without recycled materials and wood flour had a serious crushing failure with peripheral shedding. Both samples were crushed into blocks of different sizes. Therefore, with an increase in the strain rate, the fracture degree of the FMOCM was more intense, and the number of small particles increased. By collecting fragments from T#04 and O#04 after the tests, it was found that the fragments had obvious self-similarity using standard sieves of 0.00625, 0.0125, 0.25, 0.50, 0.75, 1.00, 1.50, 2.00, 3.00, 4.00, and 5.00 mm to screen the broken particles of the FMOCMs, which can be explained by fractal theory. The screening results are shown in Figs. 9 and 10. The weighted average value

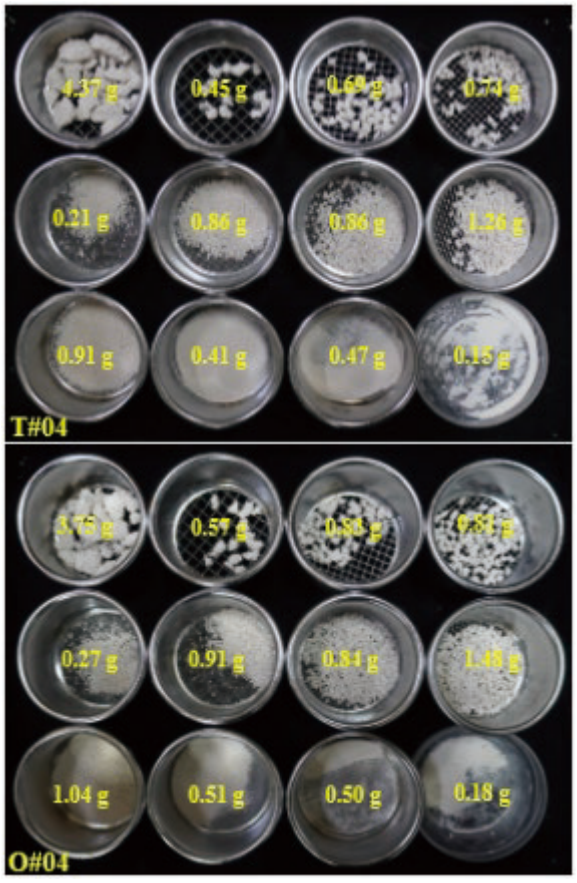


**Fig. 9.** Results and classification of fragments.

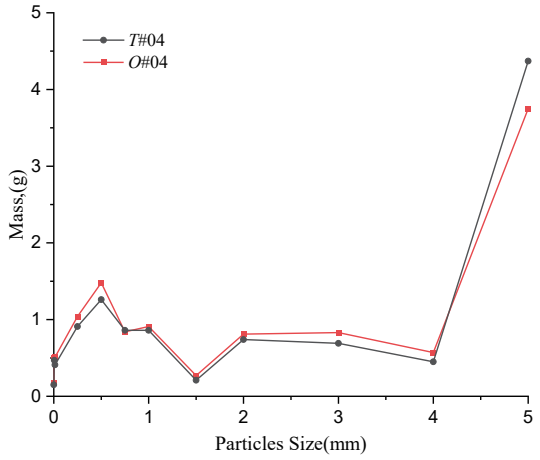


**Fig. 10.** Statistical curves of screening results.

of each particle size content was taken as the average fragmentation degree $d_m$ of an FMOCM after screening and is defined as

$$d_m = \frac{\sum (r_i d_i)}{\sum r_i} \tag{13}$$

where $d_i$ is the corresponding mesh size of each particle size, and $r_i$ is the cumulative percentage of the mass of each particle size.

Based on the screening results shown in Fig. 10 and Eq. (13), the $d_m$ of the FMOCMs with and without solid waste materials were 2.72 and 2.73 mm, respectively. Both average fragmentation degrees were basically the same, indicating that the recycled materials and wood flour did not improve the toughness of the material at high strain rates (≥400 $s^{-1}$) but replaced some natural mineral materials.

## 4 Conclusions

The effects of solid waste materials on the properties of FMOCM were investigated through mechanical and screening tests. The results showed that the internal pore microstructures of the FMOCM underwent significant changes, and the pore sizes were reduced by half owing to the addition of recycled materials and wood flour that greatly improved the quasi-static strength of the FMOCM by 54%. For the regular FMOCM, the dynamic strength almost doubled and exhibited an obvious strain rate effect. However, the addition of solid waste materials weakened the strain rate effect. According to fractal theory, the fragment degree of the FMOCMs exhibited obvious similarities at high strain rates. When the strain rate was 270 $s^{-1}$ or less, the FMOCM with solid waste materials showed better toughness compared to the more serious fracture of the regular FMOCM. Consequently, magnesium oxysulfide cementitious materials are promising candidates for preparing high-performance building materials using solid waste materials.

## Acknowledgements

This work was supported by the National Science Foundation of China (12102428), Fundamental Research Funds for the Central Universities (WK2090000019, YD2480002002,


DOI: 10.52396/JUSTC-2021-0233
*JUSTC*, **2022**, 52(4): 6

WK2480000008), and Open Research Fund of Anhui Province Key Laboratory of Green Building and Assembly Construction, Anhui Institute of Building Research & Design ( 2021-JKYL-005).

## Conflict of interest

The authors declare that they have no conflict of interest.

## Biographies

**Xiaofei Yi** is currently a master student at the Department of Modern Mechanics, University of Science and Technology of China. His research focuses on impact dynamics and mechanical behavior and design of materials.

**Yongliang Zhang** is currently an Associate Professor at the Department of Modern Mechanics, University of Science and Technology of China. His research focuses on impact dynamics and mechanical behavior and design of materials.

## References

[1] Demediuk T, Cole W F A. Study of magnesium oxy-sulphates. *Australian Journal of Chemistry,* **1957**, *10* (2): 287–294.

[2] Kahle K. Mechanism of formation of magnesium sulphate cement. *Silikattecnic,* **1972**, *23* (5): 148–1451.

[3] Urwongse L, Sorrell C A. Phase mlationships in magnesium oxysulfate cements. *Journal of the American Ceramic Society,* **1980**, *63* (03): 523–526.

[4] Zheng A R, Zhan B G, Yang Y S. Influence of mass ratio of MgO to $MgSO_4$ and $H_2O$ to $MgSO_4$ on the properties of magnesium oxysulfate cementitious material. *Journal of Hefei University of Technology (Natural Science),* **2020**, *43* (10): 1378–1383.

[5] Ma J, Yu Z Q, Ni C X, et al. Effects of limestone powder on the hydration and microstructure development of calcium sulphoaluminate cement under long-term curing. *Construction and Building Materials,* **2019**, *199*: 688–695.

[6] Liu H T, Yu Y J, Liu H M, et al. Hybrid effects of nano-silica and graphene oxide on mechanical properties and hydration products of oil well cement. *Construction and Building Materials,* **2018**, *191*: 311–319.

[7] Zhang H, Feng P, Li L, et al. Effects of starch-type polysaccharide on cement hydration and its mechanism. *Thermochimica Acta,* **2019**, *678*: 178307.

[8] Nguyen T T, Waldmann D, Bui T Q. Phase field simulation of early-age fracture in cement-based materials. *International Journal of Solids and Structures,* **2020**, *191-192*: 157–172.

[9] Wang N. Effects of sodium citrate and citric acid on the properties of magnesium oxysulfate cement. *Construction and Building Materials,* **2018**, *169*: 697–704.

[10] Yuan Q, Zhou D J, Huang H, et al. Structural build-up, hydration and strength development of cement-based materials with accelerators. *Construction and Building Materials,* **2020**, *259*: 119775.

[11] Wu C, Yu H, Zhang H, et al. Effects of phosphoric acid and phosphates on magnesium oxysulfate cement. *Materials and Structures,* **2015**, *48* (4): 907–917.

[12] Martini F, Borsacchi S, Geppi M, et al. Monitoring the hydration of MgO-based cement and its mixtures with portland cement by 1 H NMR relaxometry. *Microporous and Mesoporous Materials,* **2018**, *269*: 26–30.

[13] Husain A, Kupwade-Patll K F, Al-Aibani A, et al. In situ electrochemical impedance characterization of cement paste with volcanic ash to examine early stage of hydration. *Construction and Building Materials,* **2017**, *133*: 107–117.

[14] Wu C Y. The hydration mechanism and performance of modified magnesium oxysulfate cement by tartaric acid. *Construction and Building Materials,* **2017**, *144*: 516–524.

[15] Guan Y, Hu Z Q, Zhang Z H, et al. Effect of hydromagnesite addition on the properties and water resistance of magnesium oxysulfate (MOS) cement. *Cement and Concrete Research,* **2021**, *143*: 106387.

[16] Chen C, Wu C Y, Zhang H F, et al. Experimental study on the preparation and properties of a novel foamed concrete based on basic magnesium sulfate cement. *Bulletin of the Chinese Ceramic Society,* **2018**, *37* (3): 1022–1027.

[17] Zong J P, Liu P P, Wu C Y, et al. Study of fiber on performance of magnesium oxysulfide cement foam concrete. *China Concrete and Cement Products,* **2020**, *9* (9): 52–56.

[18] Kuzielova E, Pach L, Palou M. Effect of activated foaming agent on the foam concrete properties. *Construction & Building Materials,* **2016**, *125* (30): 998–1004.



DOI: 10.52396/JUSTC-2021-0233
*JUSTC*, **2022**, 52(4): 6